Structural Changes of Mitochondrial Creatine Kinase upon Binding of ADP, ATP, or Pi, Observed by Reaction-Induced Infrared Difference Spectra†

Thierry Granjon,‡ Marie-Jeanne Vacheron,‡ Christian Vial,*,‡ and René Buchet§

Laboratoire de Biomembranes et Enzymes Associés and Laboratoire de Physico-Chimie Biologique, UMR 5013 "Reconnaissance et Transduction Moléculaires", Université Claude Bernard Lyon 1, 69622 Villeurbanne Cedex, France

Received November 6, 2000; Revised Manuscript Received December 26, 2000

ABSTRACT: Structural modifications of rabbit heart mitochondrial creatine kinase induced by the binding of its nucleotide substrates and Pi were investigated. Reaction-induced difference spectra (RIDS), resulting from the difference between infrared spectra recorded before and after the photorelease of a caged ligand, allow us to detect very small variations in protein structure. Our results indicated that the protein secondary structure remained relatively stable during nucleotide binding. Indeed, this binding to creatine kinase affected only a few amino acids, and caused small peptide backbone deformations and alterations of the carbonyl side chains of aspartate or glutamate, reflecting modifications within preexisting elements rather than a net change in secondary structure. Nonetheless, MgADP and MgATP RIDS were distinct, whereas the MgPi RIDS presented some similarities with the MgATP one. The difference between MgADP and MgATP RIDS could reflect a distinct configuration of the two metal−nucleotide complexes inducing a different positioning and/or a distinct binding mode to the creatine kinase active site. Comparison of the MgATP and MgPi RIDS suggests that Pi binding took place at the same binding site as the γ-phosphoryl group of ATP. Thus, the difference between MgADP and MgATP RIDS would mainly be due to the effect of the γ-P of ATP. The differences observed when comparing the RIDS resulting from the binding of nucleotides to octameric mitochondrial creatine kinase or dimeric cytosolic isoform could reflect the distinct oligomerization states and physicochemical or kinetic properties of the two isoenzymes.

Members of the creatine kinase (CK)[1] isoenzyme family are tissue-specifically expressed as three cytosolic dimers and two mitochondrial isoenzymes (mtCK). The latter can exist either as dimers or as octamers (*1, 2*). The octameric form of mtCK specifically binds to the outer surface of the mitochondrial inner membrane in close proximity to the contact sites with the outer membrane (*1*−*4*). The complex, made up of mtCK, the inner mitochondrial membrane adenylate translocator, and the outer membrane porin, constitutes one side of a shuttle which efficiently exports energy as phosphocreatine (PCr) into the cytosol (*5, 6*). In addition, mtCK could play a role in the closing of the mitochondrial permeability pore which is involved in apoptosis (*7, 8*). It has long been recognized that a conformational change is induced by the interaction of the nucleotide substrates with CK (*9*−*13*).

This conformational change is of importance since it could be linked to both the dissociation of the octamer of mtCK in dimers and the solubilization of the protein from the mitochondrial membrane (*1, 2, 14*).

To obtain detailed information about the effect of substrate fixation on the structure of the mitochondrial creatine kinase isoform, we used difference infrared spectra induced by the binding of ATP, ADP, or Pi photoactivable analogues. Infrared spectroscopy allows us to visualize very small variations in protein secondary structure, especially changes in the length and geometry of bonds due to interactions with ligands or the environment. Unfortunately, the strong water absorbance in the amide I region, buffer subtraction, and different sample concentrations considerably impede spectral analysis and make small changes difficult to detect.

Difference infrared spectroscopy with photolysis of caged compounds avoids the above-mentioned uncertainties. Caged compounds, which are often substrate analogues, contain a photolabile group. Due to the chemical modification, the modified substrate cannot bind correctly to the enzyme in the dark. After photolysis, the substrate is released from its cage and can interact with the enzyme (*15, 16*). The photolysis mechanism has been previously described (*17*−*19*).

By measuring the difference infrared spectra corresponding to the dark state and to the state after illumination, it becomes possible to measure directly the effects of substrate binding to the protein. This approach avoids the problem of subtracting buffer and enables us to compensate accurately the overall spectrum of the protein which has not been affected by substrate binding, as in the Ca^{2+} ATPase of the sarco-

† This work was supported by grants from the Région Rhône-Alpes and the CNRS program "Physique et Chimie du Vivant".

* To whom correspondence should be addressed at the Laboratoire de Biomembranes et Enzymes Associés, Université Claude Bernard Lyon 1, 43 boulevard du 11 novembre 1918, F-69622 Villeurbanne Cedex, France. Tel: 33-(0) 4-72-44-82-48; Fax: 33-(0) 4-72-43-15-57; E-mail: christian.vial@univ-lyon1.fr.

‡ Laboratoire de Biomembranes et Enzymes Associés.

§ Laboratoire de Physico-Chimie Biologique.

[1] Abbreviations: CK, creatine kinase; mtCK, mitochondrial creatine kinase; Cr, creatine; DTT, dithiothreitol; FTIR, Fourier transform infrared spectroscopy; PCr, phosphocreatine; RIDS, reaction-induced difference spectrum.

10.1021/bi002553s CCC: $20.00
Published on Web 02/07/2001

plasmic reticulum (*20*−*22*), the chaperonin groEL (*23*), the nicotinic acetylcholine receptor (*24*), and the cytoplasmic creatine kinase isoform (MMCK) (*13*).

In this paper, we report new results on the effect of substrate binding to recombinant rabbit heart sarcomeric mtCK. More precisely, we demonstrate that the structural changes, caused by substrate binding, are due to the deformation of the peptide backbone and of the carboxylate side chains of Asp or Glu. Comparison of these results with others obtained on the isoforms of CK provides further insight into certain aspects of phosphoryl transfer.

MATERIALS AND METHODS

Materials. Rabbit heart mitochondrial creatine kinase was prepared and purified as previously described (*25*). The purity of CK was established by using high-resolution gel electrophoresis. Deuterium oxide (99.9% isotopic purity) was purchased from Merck. Caged nucleotides (ATP [Et-($PhNO_2$)], ADP [Et($PhNO_2$)], and Pi [Et($PhNO_2$)]) were obtained from Molecular Probes, and creatine (Cr) and phosphocreatine (PCr) were from Sigma. Tris was purchased from Boehringer Mannheim.

Infrared Spectra. MtCK (300 μg) was first lyophilized and then dissolved in ^2H_2O buffer (30 μL) in order to obtain a 10 mg/mL concentration. The final Tris-HCl concentration in buffer was 100 mM, p^{2}H 7.4. When required, 2 mM caged nucleotide, 10 mM $MgCl_2$, and 5 mM DTT with or without either 20 mM Cr or PCr were added to the sample. The p^{2}H was measured with a glass electrode and was corrected by a value of 0.4 according to Glasoe and Long (*26*).

Freshly prepared samples were loaded between two CaF_2 circular cells, with a 50 μm Teflon spacer, and incubated for 10 min in the dark at 30 °C prior to Fourier transform infrared (FTIR) spectroscopy measurement. FTIR spectra were recorded with a Nicolet 510 M FTIR spectrometer which was continuously purged with dry air. The infrared cell was thermostated with a water circulation bath. The nominal spectral resolution was 4 cm^{-1}, and 128 scans were collected during about 2 min, co-added, and Fourier-transformed. Three series of scans were recorded; then each sample was illuminated for 1 min by means of a 150 W xenon lamp (without filter) to induce the photolysis of the nucleotide from its cage. Three other series of scans were recorded between 5 and 15 min after illumination; they were superimposable, indicating that the final equilibrium was reached very rapidly due to high CK concentration (10 mg/mL). The reaction-induced difference spectrum (RIDS) of the sample was obtained by subtracting the spectrum before illumination from that after illumination. The experiment was repeated for three different samples; thus, each presented difference spectrum resulted from nine measurements to obtain a better signal-to-noise ratio. The final RIDS was corrected for water-vapor absorption.

Number of Amino Acid Residues Involved in Ligand Binding to MtCK. MtCK contains 380 amino acids giving rise to 380 carbonyl groups of the peptide backbone absorbing in the amide I region. Furthermore, 34 Arg, 16 Asn, 13 Gln, and 12 Tyr can contribute in this region with their guanidinium, amide, or phenyl groups. Therefore, the total number of absorbing groups is 455. Assuming that each group absorbs with the same molar coefficient, the number of absorbing groups (n) for a given RIDS was calculated from the COBSI index according to Barth et al. (*27*):

$$n = 0.5(455 \times \Delta A)/A$$

where A was the area of the amide I band on the original infrared spectrum of mtCK and ΔA was the sum of the integrated positive and negative difference bands between 1700 and 1600 cm^{-1} in the RIDS.

This estimation is a lower limit of the number of amino acid residues involved in the secondary structural changes (*27*, *28*). Indeed it does not take into account the overlap of initial and final bands which could occur when the shift is small and the bandwith is large.

RESULTS

Binding of MgADP to MtCK. The interaction between mtCK and its substrates is monitored by triggering the release of the ligand from an inactive photolabile caged analogue with a UV flash, without disturbing the sample. The spectrum recorded before sample illumination is the reference and is subtracted from the spectrum obtained after the release of the ligand from the cage. Thus, positive bands refer to the conformation of the substrate-bound protein and to reaction products, whereas negative signals characterize the free protein in its initial state as well as the initial substrate.

Figure 1 shows the reaction-induced difference spectrum (RIDS) of mtCK with caged ADP (trace a). The RIDS obtained with caged ADP without mtCK is shown in trace b. Despite the small absorbance of the bands, difference spectra from different samples show reproducible signals at the same wavenumbers and with comparable amplitudes. We can reasonably assume that the absorbance changes observed reflect the molecular processes of caged substrate photolysis and the conformational changes which are associated with the binding of the photolyzed substrate.

A negative band at 1529 cm^{-1} and a positive one at 1685 cm^{-1} (Figure 1, traces a and b) were related to chemical modifications which occur upon cage photolysis, that is to say, the conversion of a NO_2 group to a NO group while a C═O bond is formed. The 1529 cm^{-1} minimum corresponds to the asymmetrical stretching vibration of the disappearing nitro group of caged ADP, while the positive peak at 1685 cm^{-1} reflects the formation of the keto group of the nitrosoacetophenone (*20*, *29*).

Any other modification of the 1800−1500 cm^{-1} region is attributable to structural changes of the protein caused by nucleotide binding. Figure 1, trace c, shows the difference spectrum of the protein in the presence of ADP obtained after removing the contribution of the difference spectrum of photolysis of caged ADP (trace a minus trace b). This enabled us to detect a new negative band at around 1689−1681 cm^{-1}, which provides a better explanation for the decrease in intensity of the 1685 cm^{-1} peak (Figure 1, trace a). In addition, we observed other bands, at 1671−1668 cm^{-1} (+), 1650 cm^{-1} (−), 1638 cm^{-1} (+), 1628 cm^{-1} (−), 1618 cm^{-1} (+), 1609−1611 cm^{-1} (−), 1595 (+) cm^{-1}, 1575 cm^{-1}, and 1549−1548 cm^{-1} (−), resulting from the binding of ADP to mtCK and that correspond to the conformational alteration of the protein.

The RIDS in the 1700−1600 cm^{-1} region is characterized by a W-like shape with maxima at 1671−1668, 1638, and

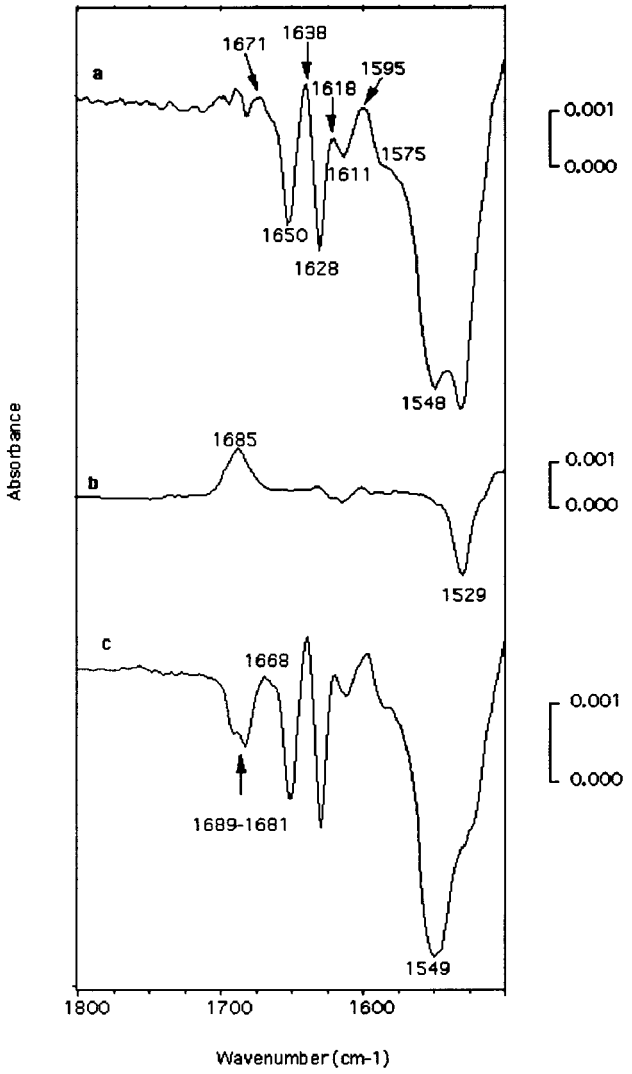

FIGURE 1: RIDS of mtCK induced by caged-ADP photolysis. (a) RIDS of ^2H_2O buffer, 100 mM Tris-HCl, p^{2}H 7.4, 2 mM caged ADP, 10 mM $MgCl_2$ in the presence of 10 mg/mL mtCK. (b) RIDS of ^2H_2O buffer, 100 mM Tris-HCl, p^{2}H 7.4, 2 mM caged ADP, 10 mM $MgCl_2$. (c) Difference spectrum between (a) and (b).

1618 cm^{-1}, and minima at 1650 and 1628 cm^{-1}. These bands located in the amide I region indicate that different secondary structure elements are involved in nucleotide binding to mtCK. Variations in the 1595−1575 cm^{-1} region suggest that carboxylates were affected by nucleotide binding.

Binding of MgADP to MtCK in the Presence of DTT. 2-Nitrosoacetophenone, which is released after photolysis, is liable to react with the cysteine residues and can therefore inactivate or modify the protein. Reduced thiols, such as DTT or glutathione, can scavenge this nitrosoketone. Indeed, addition of DTT displaced the photolysis signal from 1685 cm^{-1} to about 1640 cm^{-1} (not shown), that was interpreted as an interaction between the carbonyl group of the nitrosoketone and the thiol group (*18*). Apart from this modification, the RIDS of mtCK in the presence of DTT is unchanged, suggesting that the 2-nitrosoacetophenone itself does not affect the active site, as already demonstrated in the case of cytosolic CK (*30*).

Binding of MgADP to MtCK in the Presence of PCr or Cr. Since infrared samples require a high protein concentration (10 mg/mL), thus increasing protein−protein interactions, it is important to ensure that the activity of the analyzed sample is not affected. As previously indicated, mtCK catalyzes the reversible transfer of a phosphoryl group from PCr to MgADP, generating creatine and MgATP. Thus, infrared spectra were recorded in the presence of mtCK and PCr. Addition of caged ADP, in the dark, does not induce any transfer, in contrast to the events following illumination. RIDS of mtCK in the presence of MgADP + PCr (reactive medium) exhibited intense positive peaks at 1622 and 1576 cm^{-1} and two negative peaks at 1607 and 1548 cm^{-1} (Figure 2 A). As previously shown, the absorption spectrum of creatine in ^2H_2O showed two positive bands at 1618 and 1576 cm^{-1}, whereas the absorption spectrum of phosphocreatine showed two positive bands located at 1609 and 1548 cm^{-1} (*30*). Therefore, the modifications we observed are obviously associated with the transformation of PCr and ADP to Cr and ATP. Photolysis-induced ADP release led to the activation of phosphoryl transfer from PCr to ADP with Cr and ATP formation, indicating that mtCK was active under these conditions. In addition, subtle changes took place in the amide I region that were interpreted mainly as nucleotide binding effects.

For comparison, RIDS of mtCK, in the presence of caged ADP and Cr (i.e., nonreactive medium), is shown in Figure 2B. The spectral changes in the amide I region were dominated by the effects of nucleotide binding (see, for example, Figure 1, trace a), and no phosphoryl transfer occurred.

To better evaluate the structural effects of PCr and Cr, respectively, on mtCK, the difference between the two RIDS [(RIDS of mtCK + PCr + caged ADP) − (RIDS of mtCK + Cr + caged ADP)] was calculated (Figure 2C). This difference spectrum confirmed the phosphoryl transfer from PCr to ADP, as indicated by the two positive peaks at 1624−1628 and 1576 cm^{-1} as well as by the two negative peaks at 1607 and 1548 cm^{-1}. It is quite similar to the infrared spectrum of creatine minus the infrared spectrum of PCr shown in Figure 2D. In addition, a small band was observed around 1651 cm^{-1} which can be assigned to the difference in the binding of ADP (1651 cm^{-1} more intense) and of ATP produced during the phosphoryl transfer from PCr to ADP.

Binding of MgADP to MtCK in the Presence of Cr, or in the Transition-State Analogue Complex. The extremely stable transition-state analogue complex of mtCK, formed with creatine, MgADP, and planar anions such as NO_3^-, mimicks the intermediate state of the phosphoryl transfer process (*31*). The RIDS of mtCK in the presence of Cr (Figure 2B) and in a transition-like state (Figure 3) are similar to the RIDS of mtCK with caged ADP alone (Figure 1, trace a). This indicates that Cr binding to mtCK, and also the transition state, did not induce detectable structural changes in addition to those observed with MgADP. Thus, changes observed in RIDS are mainly due to nucleotide binding.

Binding of MgATP or MgPi to MtCK. The binding of MgATP or MgPi to mtCK leads to RIDS which present some similarities (Figure 4, traces a and b). RIDS always show the photolysis bands at 1529 and 1685 cm^{-1} associated with the transformation of caged substrates, but the W-like shape in the amide I region characterizing ADP binding (Figure 1, trace a) did not appear in the case of ATP or Pi binding. Figure 4, traces a and b, exhibited minima at around 1547, 1611, and 1651 cm^{-1}, one major maximum around

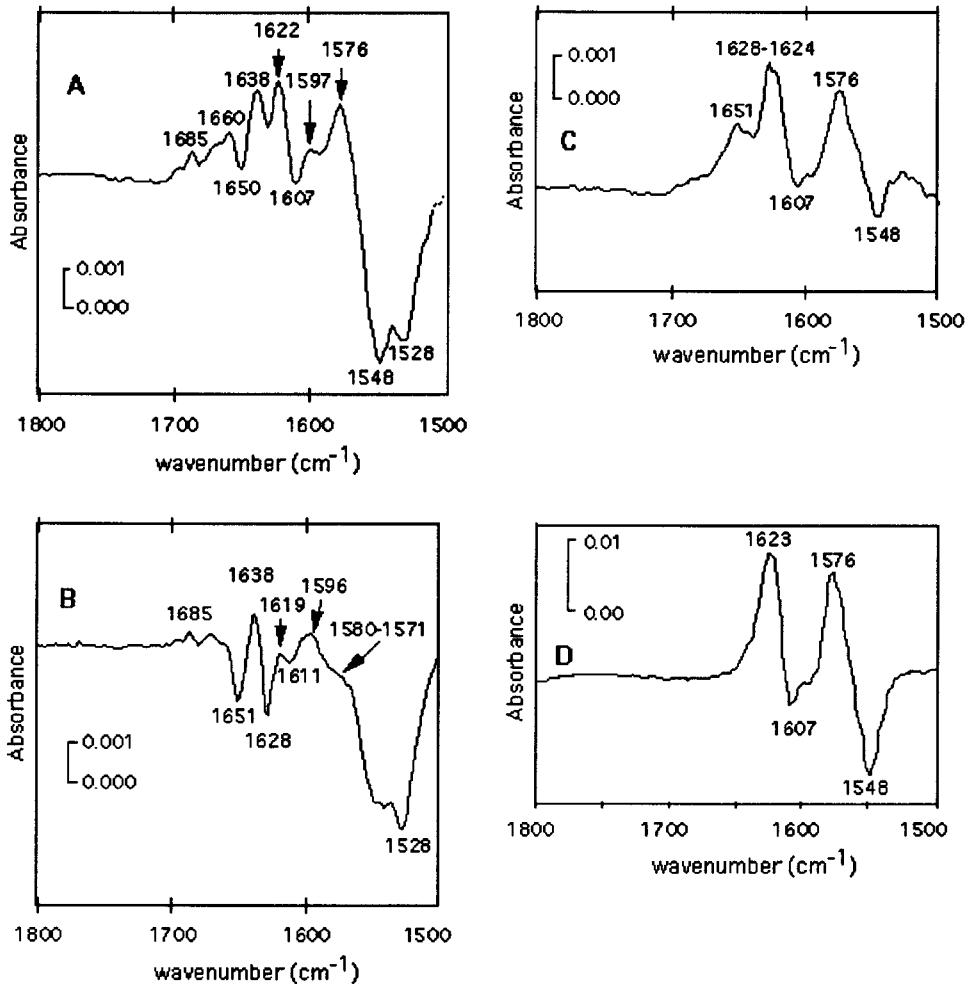

FIGURE 2: RIDS of mtCK induced by caged-ADP photolysis in a reactive or nonreactive medium. (A) RIDS of ^2H_2O buffer, 100 mM Tris-HCl, p^{2}H 7.4, 2 mM caged ADP, 10 mM $MgCl_2$ in the presence of 10 mg/mL mtCK and 20 mM PCr (reactive medium). (B) RIDS of ^2H_2O buffer, 100 mM Tris-HCl, p^{2}H 7.4, 2 mM caged ADP, 10 mM $MgCl_2$ in the presence of 10 mg/mL mtCK and 20 mM Cr (nonreactive medium). (C) Difference spectrum between (A) and (B). (D) Infrared spectrum of 20 mM Cr minus infrared spectrum of 20 mM PCr in ^2H_2O buffer, 100 mM Tris-HCl, p^{2}H 7.4, 10 mM $MgCl_2$.

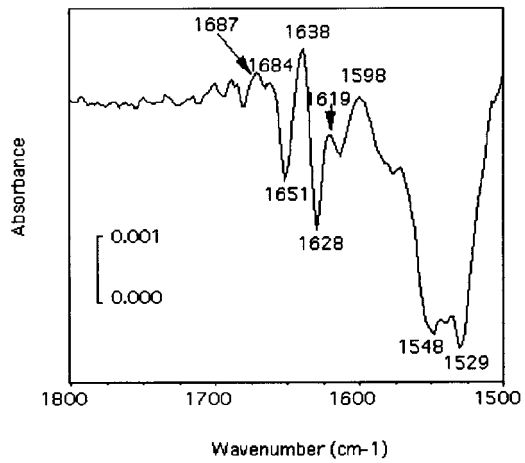

FIGURE 3: RIDS of mtCK in the transition-like state induced by caged-ADP photolysis. RIDS of ^2H_2O buffer containing 100 mM Tris-HCl, p^{2}H 7.4, 2 mM caged ADP, 10 mM $MgCl_2$, 40 mM Cr, 50 mM KNO_3, with 10 mg/mL mtCK.

1624 cm^{-1}, and minor positive bands around 1638 and 1600 cm^{-1}. The main differences between the RIDS of mtCK + ATP or Pi and the RIDS of mtCK + ADP were the absence of the 1628 cm^{-1} negative peak and the presence of a 1624 cm^{-1} positive one.

The RIDS of mtCK + caged ATP + PCr (Figure 5, trace a) was almost identical to the RIDS of mtCK + caged ATP (Figure 4, trace a), suggesting that PCr does not induce additional structural changes. Results obtained in the case of caged Pi with mtCK and either Cr or PCr (Figure 5, traces b and c) did not produce additional bands, but the relative magnitudes of infrared difference bands were slightly affected.

Binding of MgATP to MtCK in the Presence of Cr. As expected for a reversible active system, addition of Cr and MgATP to mtCK leads to the formation of PCr and the disappearance of Cr, indicated by a decrease in the 1623 and 1576 cm^{-1} bands and an increase in the 1607 and 1548 cm^{-1} ones, as already discussed (not shown). However, the observed changes are very slight with respect to those observed in the case of the reverse reaction with MgADP and PCr (Figure 2A). These small changes are consistent with those expected from the value of the equilibrium constant of CK.

DISCUSSION

We measured difference infrared spectra combined with light-induced photolysis of caged compounds to monitor the effects of ADP, ATP, or Pi binding on mtCK structure.

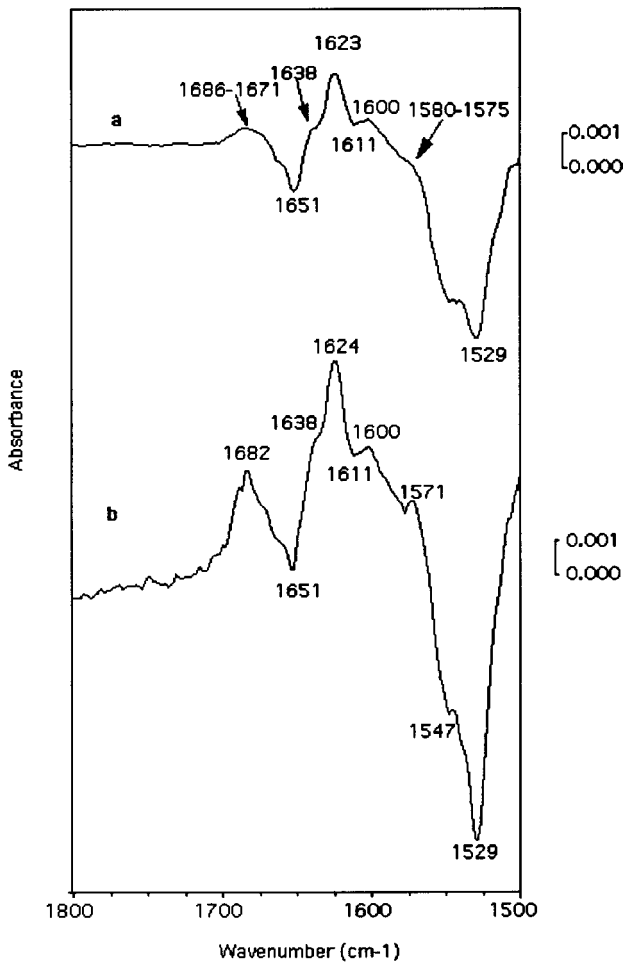

FIGURE 4: RIDS of mtCK induced by the release of ATP or Pi from their cage. (a) RIDS of ^2H_2O buffer, 100 mM Tris-HCl, p^{2}H 7.4, 2 mM caged ATP, 10 mM $MgCl_2$ in the presence of 10 mg/mL mtCK. (b) RIDS of ^2H_2O buffer, 100 mM Tris-HCl, p^{2}H 7.4, 2 mM caged Pi, 10 mM $MgCl_2$ in the presence of 10 mg/mL mtCK.

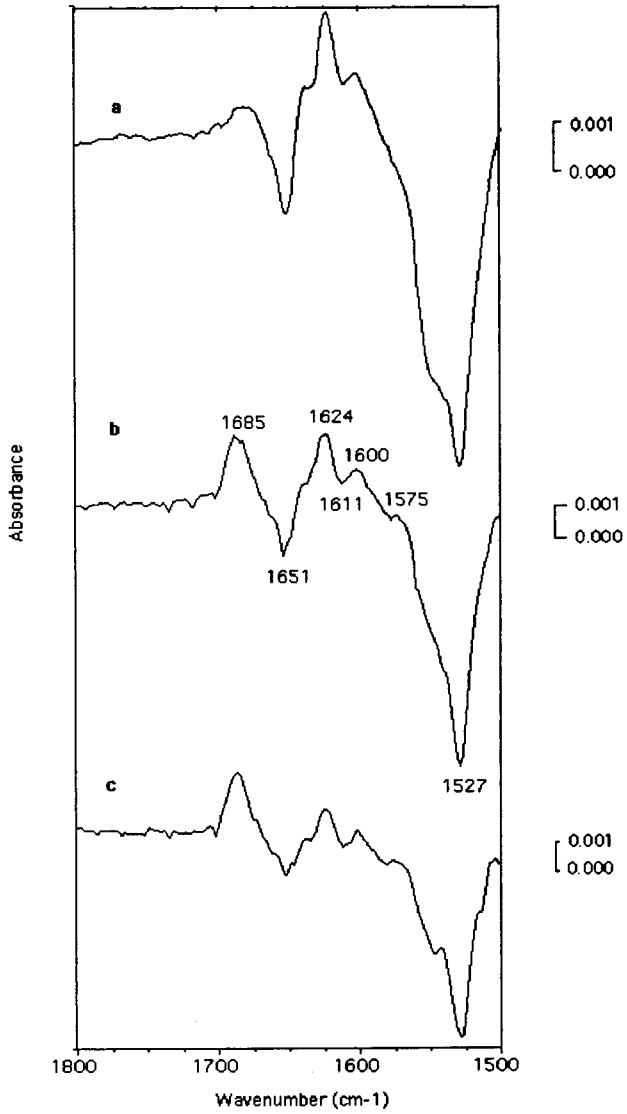

FIGURE 5: RIDS of mtCK induced by the release of ATP or Pi in the presence of either PCr or Cr. (a) RIDS of ^2H_2O buffer, 100 mM Tris-HCl, p^{2}H 7.4, 2 mM caged ATP, 10 mM $MgCl_2$, 20 mM PCr with 10 mg/mL mtCK. (b) RIDS of ^2H_2O buffer, 100 mM Tris-HCl, p^{2}H 7.4, 2 mM caged Pi, 10 mM $MgCl_2$, 20 mM Cr in the presence of 10 mg/mL mtCK. (c) RIDS of ^2H_2O buffer, 100 mM Tris-HCl, p^{2}H 7.4, 2 mM caged Pi, 10 mM $MgCl_2$, 20 mM PCr in the presence of 10 mg/mL mtCK.

Caged compounds enabled us to record the same sample before and after substrate release by photolysis, increasing the sensitivity and reproducibility of difference spectra (*32*). The highly reproducible mtCK changes in the difference spectra provided evidence of a structural change upon nucleotide binding.

However, the recorded spectra may be subject to several artifacts. These artifacts could arise from possible radiation damage, interaction of the photolysis byproducts with mtCK, or reaction-induced denaturations. None of the infrared signals typical of thermal or pH denaturation of mtCK (*33*) were observed, suggesting that there was no radiation damage caused by the photolysis process. The inhibition of activity and the photolysis−product interaction with the enzyme could be prevented by the addition of DTT (*17*). This addition did not induce any significant shift in the infrared signals of the protein, as we have already shown in the case of cytosolic MMCK (*30*). Thus, the changes observed on RIDS are unlikely to be related to the previously mentioned artifacts. However, DTT can be rapidly oxidized and is then liable to interact with the reactive Cys_{278} in the mtCK active site and to induce a modification of the protein RIDS (*34*). For such reasons, DTT was not added systematically to our samples. Accordingly, the observed RIDS resulted from slight structural changes of mtCK together with those caused by cage photolysis. Comparison of spectra obtained in the presence and in the absence of protein allowed us to separate both contributions. Bands at 1685 and 1524−1529 cm^{-1} were assigned to photolysis products, in agreement with the literature data (*18*). All other bands were therefore attributed to structural protein modifications.

Comparison of RIDS of mtCK with MgADP, MgATP, or MgPi indicated that each substrate had a specific effect on the protein conformation, inducing small structural alterations of mtCK upon nucleotide or Pi binding.

ADP Binding. The strongest difference bands of mtCK with MgADP (Figure 1) were signals at 1650 cm^{-1} (−), 1638 cm^{-1} (+), and 1628 cm^{-1} (−) giving rise to a RIDS with a W-like shape. Less intense differential bands appear around 1689−1681 cm^{-1} (−), 1671−1668 cm^{-1} (+), 1618 cm^{-1} (+), around 1611 cm^{-1} (−), in the 1600−1560 cm^{-1} region, and at 1549−1548 cm^{-1} (−).

The assignment of these bands (as reviewed in *35*, *36*) is based on the absorption of side chain residues (*37*, *38*), amide I (*39*), and nucleotides (*40*). The band at 1650 cm^{-1} has been attributed to α-helical structure (*41*−*43*). Other differential signals between 1700 and 1600 cm^{-1} were characteristic of β sheets (1690, 1638, and 1628 cm^{-1}). However, the overall absorbance changes in the amide I region were very small; the RIDS intensity allowed us to give an approximate lower estimation of the number of implicated residues (see Materials and Methods). We recorded only slight changes involving at least two to three carbonyl peptide backbones per mtCK monomer. This suggests that the conformational changes induced in mtCK upon nucleotide binding might reflect modifications within preexisting secondary structure elements, like compression or dilation, rather than a net change in secondary structure (*27*).

The 1600−1560 cm^{-1} region probably corresponded to the absorption of the ionized carboxylate residues of Asp or Glu (*37*, *38*), suggesting an interaction between carboxylate residue(s) and Mg-nucleotide. One could speculate about the position of the implicated carboxylate residue(s). Crystallographic data suggest that the adenine base of nucleotides fits into a pocket comprising residues Met_{235}, His_{186}, Ser_{123}, His_{291}, Gly_{289}, Arg_{125}, Arg_{287}, and Asp_{330} (*44*). Asp_{330} is located nearby the adenosine moiety and thus could establish hydrogen bonds with adenosine. Such an interaction has not been observed in the crystallographic structure, but it should be remembered that the nucleotide is not in its correct position in this case (*45*). The Asp_{330} residue is in close proximity to Asp_{327} and to the flexible and protease-sensitive loop Gly_{316}−Ala_{326}, which contains another acidic residue, Asp_{321}. This loop is believed to close the site upon nucleotide fixation (*46*). Alternatively, it was proposed that Glu_{226}, Glu_{227}, and Asp_{228} could be involved in coordinating the Mg^{2+} of the nucleotides in mtCK (*44*). Finally, there is evidence from reactive analogues of the presence of two other carboxylates close to the nucleotide binding domain, Asp_{335} and Glu_{236} (*47*, *48*).

The amide II band located around 1548 cm^{-1} corresponded to the NH groups of the peptide backbone. The variations in the intensity of this band are mostly related to the extent of the H/^{2}H exchange rate of the NH groups with ^2H_2O molecules, indicating that nucleotide binding to mtCK displaced some NH groups which were not easily accessible to water in the initial protein state. Wyss proposed that the nucleotide binding domain of mtCK is close to the hinge region of the enzyme (*46*), so that some domains of the protein could move upon nucleotide binding, consistent with the described flexible loops of the enzyme (*44*, *49*).

ATP and Pi Binding. The binding of either MgATP or MgPi to mtCK (Figure 4, traces a and b) gives rise to RIDS with similar positions of positive and negative peaks, although the magnitudes of the peaks may differ. However, these spectra were different from those obtained with MgADP (Figure 1, trace a). The W-like profile observed in the amide I region with ADP does not appear with either ATP or Pi. ATP and Pi difference spectra presented only two major peaks at 1651 cm^{-1} (−) and 1624 cm^{-1} (+), and less intense bands at 1638 cm^{-1} (+), around 1611 cm^{-1} (−), and at 1547 cm^{-1} (−).

These results demonstrated distinct structural alterations caused by ADP and ATP binding to mtCK. The difference of behavior between MgADP and MgATP would be due to the distinct configuration of these two complexes. As shown by NMR results on the conformation of metal−nucleotide complexes bound to cytosolic CK, Mg^{2+} forms a tridentate complex with α, β, and γ-P of ATP, leading to a particular configuration which allows for a specific position of Mg^{2+} and ATP γ-P in the active site, whereas the bidentate complex between Mg^{2+} and the α and β-P of ADP leads to a different positioning of the cation and phosphoryl groups (*50*). Furthermore, it could be suggested that the strong positive signal observed at 1624 cm^{-1} in RIDS of both MgPi and MgATP results from the binding of MgPi to the same position as the γ-P of ATP, although Pi binding to other sites giving rise to minor infrared signals cannot be excluded. The differences between the RIDS of ATP and ADP could originate from the prevalence of the Pi-like infrared signal of the γ-P of ATP on that of the ADP moiety of ATP.

Nucleotides Binding to MtCK in the Presence of either PCr, Cr, or the Transition-State Analogue. The functionality of the system was verified for phosphoryl transfer. We induced the enzymatic reaction by the addition of MgADP or MgATP to mtCK in the presence of PCr or Cr, respectively. The light-induced nucleotide release activated phosphoryl transfer, as probed by the infrared changes related to the reversible transformation of PCr to Cr. The observed difference spectra correspond to the simultaneous presence of MgADP, MgATP, Cr, and PCr at equilibrium.

From experiments with Cr, PCr, or the transition-state analogue, we concluded that binding of any nucleotide to mtCK was not globally affected by the presence of either Cr or PCr since the latter did not induce any substantial additional changes in the difference spectra. The Cr or PCr binding site may be located close to the N-terminal loop of the enzyme (*51*, *52*). Furthermore, even if Cr, PCr, or the transition-state analogue induced modifications of mtCK structure, these changes did not appear on difference spectra since these substrates were added before the light-induced nucleotide release. The eventual spectral changes only provided information about the nucleotide binding effect, as well as about the coupling between substrates and the nucleotide binding site of protein.

In conclusion, structural alterations caused by Mg-nucleotide binding to mtCK are relatively small, involving only a few amino acids as probed by RIDS. This structural change of mtCK upon nucleotide binding can result from the flexibility of the secondary structure rather than from a modification of its structural element contents. This may implicate distortions of α helices, as suggested by changes around the 1650 cm^{-1} band, as well as variations in the hydrogen bonding of β-sheet structures, as indicated by the 1628 (−) and 1638 (+) cm^{-1} bands. Tertiary structure modifications induced by nucleotidic substrate binding have been evidenced by ultraviolet absorption or fluorescence spectroscopies as well as proton NMR measurements (*9*, *11*, *53*). More recently, considerable changes in the size and shape of mtCK upon binding of Mg-nucleotide or transition-state analogue complex have been demonstrated using small-angle X-ray scattering. These modifications would be related to domain motion as movements of the dimeric building blocks of the octamer (*12*). In addition, it was proposed that, after binding of Mg-nucleotide, loops 60−66 and 316−326 would move nearer the active site to exclude water molecules

during catalysis, leading to a "close conformation" of the enzyme (*44*). All these modifications would perturb the bonds implicated in the β-sheet and α-helix structures, by varying their length and geometry without significantly altering the protein secondary structure as evidenced with our RIDS results.

On the other hand, comparison of the present data with those obtained with cytosolic MMCK indicates that RIDS of MgADP are similar whereas those of MgPi and MgATP present some differences in the two isoforms. MMCK RIDS for MgATP and MgPi showed a negative peak at 1623−1625 cm^{-1} instead of a positive peak for mtCK (*13*). In the case of mtCK, the RIDS of MgATP seems to result from the summation of the MgPi infrared signal with that of MgADP, inferring that the MgPi binding site is located within the γ-ATP binding site. However, in the case of MMCK, the binding site of MgPi seems to be looser and may not be restricted to the γ-ATP binding site (*13*). This suggests that the differences between ATP RIDS of mtCK and MMCK originate in the Pi RIDS signals. These variations could reflect the differences between the oligomeric state of the octameric mtCK and the dimeric MMCK, or some of their physicochemical or enzymatic characteristics.

ACKNOWLEDGMENT

We thank Dr. O. Marcillat for stimulating discussion and for critical reading of the manuscript.

REFERENCES

1. Marcillat, O., Goldschmidt, D., Eichenberger, D., and Vial, C. (1987) *Biochim. Biophys. Acta 890*, 233−241.
2. Schlegel, J., Zurbriggen, B., Wegmann, G., Wyss, M., Eppenberger, H. M., and Wallimann, T. (1988) *J. Biol. Chem. 263*, 16942−16953.
3. Quemeneur, E., Eichenberger, D., Goldschmidt, D., Vial, C., Beauregard, G., and Potier, M. (1988) *Biochem. Biophys. Res. Commun. 153*, 1310−1314.
4. Adams, V., Bosch, W., Schlegel, J., Wallimann, T., and Brdiczka, D. (1989) *Biochim. Biophys. Acta 981*, 213−225.
5. Brdiczka, D. (1991) *Biochim. Biophys. Acta 1071*, 291−312.
6. Schlattner, U., Forstner, M., Eder, M., Stachowiak, O., Fritz-Wolf, K., and Wallimann, T. (1998) *Mol. Cell. Biochem. 184*, 125−140.
7. Beutner, G., Rück, A., Riede, B., Welte, W., and Brdiczka, D. (1996) *FEBS Lett. 396*, 189−195.
8. O'Gorman, E., Beutner, G., Dolder, M., Koretsky, A. P., Brdiczka, D., and Wallimann, T. (1997) *FEBS Lett. 414*, 253−257.
9. Roustan, C., Kassab, R., Pradel, L. A., and Van Thoai, N. (1968) *Biochim. Biophys. Acta 167*, 326−338.
10. Vasak, M., Nagayama, K., Wuthrich, K., Mertens, M. L., and Kagi, H. R. (1979) *Biochemistry 18*, 5050−5055.
11. Messmer, C. H., and Kagi, H. R. (1985) *Biochemistry 24*, 7172−7178.
12. Forstner, M., Kriechbaum, M., Laggner, P., and Wallimann, T. (1998) *Biophys. J. 75*, 1016−1023.
13. Raimbault, C., Buchet, R., and Vial, C. (1996) *Eur. J. Biochem. 240*, 134−142.
14. Brooks, S. P. J., and Suelter, C. H. (1987) *Arch. Biochem. Biophys. 253*, 122−132.
15. Kaplan, J. H., Forbush, B., and Hoffman, J. F. (1978) *Biochemistry 10*, 1929−1935.
16. McCray, J. A., Herbette, L., Kihara, T., and Trentham, D. R. (1980) *Proc. Natl. Acad. Sci. U.S.A. 77*, 7237−7241.
17. Walker, J. W., Reid, G. P., McCray, J. A., and Trentham, D. R. (1988) *J. Am. Chem. Soc. 110*, 7170−7177.
18. Barth, A., Corrie, J. E. T., Gradwell, M. J., Maeda, Y., Mäntele, W., Meie, T., and Trentham, D. R. (1997) *J. Am. Chem. Soc. 119*, 4149−4159.
19. Cepus, V., Ulbrich, C., Allin, C., Troullier, A., and Gerwert, K. (1998) *Methods Enzymol. 291*, 223−245.
20. Barth, A., Kreutz, W., and Mäntele, W. (1990) *FEBS Lett. 277*, 147−150.
21. Barth, A., and Mäntele, W. (1998) *Biophys. J. 75*, 538−544.
22. Von Germar, F., Barth, A., and Mäntele, W. (2000) *Biophys. J. 78*, 1531−1540.
23. Von Germar, F., Galan, A., Llorca, O., Carrascosa, J. L., Valpuesta, J. M., Mäntele, W., and Muga, A. (1999) *J. Biol. Chem. 274*, 5508−5513.
24. Görne-Tschelnokow, U., Hucho, F., Naumann, D., Barth, A., and Mäntele, W. (1992) *FEBS Lett. 309*, 213−217.
25. Marcillat, O., Perraut, C., Granjon, T., Vial, C., and Vacheron, M. J. (1999) *Protein Expression Purif. 17*, 163−168.
26. Glasoe, P. K., and Long, F. A. (1960) *J. Phys. Chem. 64*, 188−190.
27. Barth, A., von Germar, F., Kreutz, W., and Mäntele, W. (1996) *J. Biol. Chem. 271*, 30637−30646.
28. Raussens, V., Pézolet, M., Ruysschaert, J. M., and Goormaghtigh, E. (1999) *Eur. J. Biochem. 262*, 176−183.
29. Barth, A., Mäntele, W., and Kreutz, W. (1991) *Biochim. Biophys. Acta 1057*, 115−123.
30. Raimbault, C., Clottes, E., Leydier, C., Vial, C., and Buchet, R. (1997) *Eur. J. Biochem. 247*, 1197−1208.
31. Travers, F., and Barman, T. E. (1980) *Eur. J. Biochem. 110*, 405−412.
32. Mäntele, W. (1993) *Trends Biochem. Sci. 18*, 197−202.
33. Raimbault, C., Couthon, F., Vial, C., and Buchet, R. (1995) *Eur. J. Biochem. 234*, 570−578.
34. Buechter, D. D., Medzihradszky, K. F., Burlingame, A. L., and Kenyon, G. L. (1992) *J. Biol. Chem. 267*, 2173−2178.
35. Surewicz, W. K., and Mantsch, H. H. (1988) *Biochim. Biophys. Acta 952*, 115−130.
36. Jackson, M., and Mantsch, H. H. (1995) *Crit. Rev. Biochem. Mol. Biol. 30*, 95−120.
37. Chirgadze, Y. N., Fedorov, O. V., and Trushina, N. P. (1975) *Biopolymers 14*, 679−694.
38. Venyaminov, S. Y., and Kalnin, N. N. (1990) *Biopolymers 30*, 1243−1257.
39. Bandekar, J. (1992) *Biochim. Biophys. Acta 112*, 123−143.
40. Shimanouchi, T., Tsuboi, M., and Kyogoku, Y. (1964) *Adv. Chem. Phys. 7*, 435−496.
41. Goormaghtigh, E., Cabiaux, V., and Ruysschaert, J. M. (1994) in *Subcellular Biochemistry* (Hilderson, H. J., and Ralston, G. B. Eds.) pp 329−362, Plenum Press, New York.
42. Muga, A., Mantsch, H., and Surewicz, W. K. (1991) *Biochemistry 30*, 2629−2635.
43. Surewicz, W. K., Mantsch, H. H., and Chapman, D. (1993) *Biochemistry 32*, 389−394.
44. Fritz-Wolf, K., Schnyder, T., Wallimann, T., and Kabsch, W. (1996) *Nature 381*, 341−345.
45. Kabsch, W., and Fritz-Wolf, K. (1997) *Curr. Opin. Struct. Biol. 7*, 811−818.
46. Wyss, M., James, P., Schlegel, J., and Wallimann, T. (1993) *Biochemistry 32*, 10727−10735.
47. James, P., Wyss, M., Lutsenko, S., Wallimann, T., and Carafoli, E. (1990) *FEBS Lett. 273*, 139−143.
48. Olcott, M. C., Bradley, M. L., and Haley, B. E. (1994) *Biochemistry 33*, 11935−11941.
49. Leydier, C., Andersen, J. S., Couthon, F., Forest, E., Marcillat, O., Denoroy, L., Vial, C., and Clottes, E. (1997) *J. Protein Chem. 16*, 67−74.
50. Ray, B. D., Chau, M. H., Fife, W. K., Jarori, G. K., and Nageswara Rao, B. D. (1996) *Biochemistry 35*, 7239−7246.
51. Suzuki, T., Kawasaki, Y., Furukohri, T., and Ellington, W. R. (1997) *Biochim. Biophys. Acta 1348*, 152−159.
52. Min, K. L., Steghens, J. P., Henry, R., Doutheau, A., and Collombel, C. (1998) *Biochim. Biophys. Acta 137*, 80−88.
53. Rosevear, P. R., Desmeules, P., Kenyon, G. L., and Mildvan, A. S. (1981) *Biochemistry 20*, 6155−6164.

BI002553S